UDK 669.14.018.8
Original scientific article/Izvirni znanstveni članek

ISSN 1580-2949
MTAEC9, 57(5)475(2023)

PREDICTION OF MICROSTRUCTURE EVOLUTION OF 316LN AUSTENITIC STAINLESS STEEL USING CELLULAR AUTOMATA AND A NOVEL EVALUATION METHOD FOR GRAIN SIZE INHOMOGENEITY

NAPOVED RAZVOJA MIKROSTRUKTURE AUSTENITNEGA NERJAVNEGA JEKLA VRSTE 316LN Z UPORABO CELIČNIH AVTOMATOV IN NOVA METODA ZA OVREDNOTENJE NEHOMOGENE VELIKOSTI KRISTALNIH ZRN

Min Qin*, Jiansheng Liu

School of Materials Science and Engineering, Taiyuan University of Science and Technology, 030024 Taiyuan, China

Prejem rokopisa – received: 2023-22-15; sprejem za objavo – accepted for publication: 2023-07-28

doi:10.17222/mit.2023.796

Inhomogeneous grain size is a significant structural defect in large forgings. This study employed cellular automata to simulate the dynamic recrystallization (DRX) of 316LN steel and analyzed the grain distribution during DRX. The accuracy of the CA method was verified by comparing its results with the results of a thermal simulation test on Gleeble 1500D. Subsequently, a novel method for evaluating grain size inhomogeneity was proposed. The grain size inhomogeneity coefficient G_u was introduced to determine the evolution of grain size inhomogeneity during DRX. This coefficient accurately and objectively reflects grain inhomogeneity. The impact of the initial and recrystallized grain size on the inhomogeneity during DRX was also analyzed.

Keywords: grain size inhomogeneity, 316LN, cellular automata, evaluate

Nehomogena velikost kristalnih zrn je pomembna strukturna pomanjkljivost oziroma napaka v velikih odkovkih. V tej študiji avtorja opisujeta uporabo metode celičnih avtomatov (CA) za simulacijo procesa dinamične rekristalizacije (DRX) v nerjavnem jeklu vrste 316LN in analizo porazdelitve velikosti kristalnih zrn med DRX.Natančnost CA metode sta verificirala s primerjavo z eksperimentalnimi rezultati dobljenimi s testi termične simulacije na napravi Gleeble1500D. Nato sta avtorja raziskave predlagala novo metodo za ovrednotenje nehomogene velikosti kristalnih zrn. Uvedla sta parameter (koeficient) nehomogenosti za določitev razvoja neenakomerne velikosti kristalnih zrn med DRX. Ta koeficient se objektivno odraža v nehomogenosti kristalnih zrnin jo natančno opisuje. Avtorja sta prav tako analizirala vpliv začetne in rekristalizirane velikosti kristalnih zrna na nehomogenost med DRX.

Ključne besede: nehomogena velikost kristalnih zrn; nerjavno jeklo vrste 316LN; celični avtomati; ovrednotenje

1 INTRODUCTION

During a forging process, the distribution of grain size can become uneven due to incomplete recrystallization, the pinning effect of second-phase particles and the influence of trace elements, resulting in one of the most critical structural defects of large forgings.[1] This can cause a reduction in the yield strength, impact toughness, and overall quality and service performance.

Ryabykin et al. identified grain size macro inhomogeneity as the most negative feature of the structure of a ring fabricated from high-alloy alloys, resulting from non-uniform deformation.[2] Feng et al. investigated the effect of grain size inhomogeneity on the dynamic softening behavior and processing map of Al-8Zn-2Mg-2Cu alloy, and found that the suitable hot-deformation process for rolling large ingots should be carried out in a temperature range of 440–450 °C and at a strain rate of 0.1–0.3s^{-1}, taking into account the ingot grain size inhomogeneity.[3] Sun et al. studied the microstructure inhomogeneity of prefabricated Co-28Cr-6Mo-0.23C-0.17N alloy cylindrical bars and found that the growth of the existing ε-hcp grains increased the volume fraction of the ε-hcp phase more easily than the nucleation and growth of the new ε-hcp grains, leading to differences in the grain size.[4] Betsofen et al. used the X-ray rocking curve method (RCM) to characterize the microstructure texture of Al and its alloys and found that grains with orientations of {111} and {100} grew much faster than those with orientations of {113} and {110}, contributing to grain size inhomogeneity.[5] Landgraf et al. linked the grain size inhomogeneity of semi processed electrical steel to work hardening inhomogeneity in cold rolling of hot bands that were annealed to obtain large grain size.[6]

In the 1980s, Wolfram et al. developed the mesoscale cellular automata (CA) method, which has been widely used in material science research to simulate the microstructure evolution of various metal materials during hot

*Corresponding author's e-mail:
wsqm2008@163.com (Min Qin)

forming.[7] For example, Alavi et al. studied the static recrystallization and microstructure evolution using austenitic stainless steel 304L.[8] A microstructural-thermal model based on CA was constructed to evaluate the rate of static recrystallization within rolled steel. The static recrystallization process was analyzed by Shi et al. based on the CA method.[9] The static recrystallization behavior of LZ50 steel was accurately predicted.

Su et al. established a three-dimensional CA model to analyze the austenitization of GCr15 steel at different temperatures and under different processing times, and the degree of austenitization was predicted.[10] Iwamoto simulated the deformation behavior of the martensitic phase under plane strain condition using the CA method coupled with a formulated constitutive equation and finite element method (FEM).[11] Qian et al. investigated the microstructure evolution and plastic flow characteristics of an HY-100 steel using a simulative model that coupled the CA method with the basic metallurgical principle of dynamic recrystallization (DRX).[12] Moreover, Alavi et al. coupled an artificial neural network technique with the thermal-CA model to predict the martensite reversion, temperature history, and recrystallization progress during subsequent non-isothermal heat treatments.[13]

However, few studies have investigated specific evaluation methods for grain size inhomogeneity and may rely on metallographic photos for observation. Given that the CA method is an intuitive and accurate way to study the microstructure evolution during hot forming, this paper uses it to analyze the grain size inhomogeneity during the DRX of 316LN steel. The proposed method provides a rational approach to evaluating grain size inhomogeneity.

2 CA MODEL OF DRX AND SIMULATION

The paper focuses on studying the grain size inhomogeneity of 316LN steel during deformation, which is mainly influenced by microstructure inheritance and incomplete recrystallization. To understand this inhomogeneity, we focused on the recrystallization of 316LN steel and the associated changes in the grain size. To this end, we established a DRX model that includes nucleation, dislocation density evolution and gain growth.[15]

2.1 Modeling of DRX nucleation

Modeling of DRX nucleation can be described with Equation (1), as follows:[16,17]

$$n(e,T) = C\dot{\varepsilon}^{m} \exp\left(-\frac{Q_N}{RT}\right) \tag{1}$$

where C is the constant that can be obtained by experimentally measuring the fraction of dynamic recrystallization under specific deformation conditions, m is set to 1.0 in the present simulation, Q_N is the activation energy, $\dot{\varepsilon}$ is the strain rate, R is the universal gas constant, and T is the absolute temperature.

2.2 Modeling of dislocation density

The flow stress is proportional to the square root of dislocation density as given by Equation (2), as follows:[18,19]

$$\sigma = a\mu b\sqrt{\rho} \tag{2}$$

where α is the dislocation interaction term, $\alpha = 0.5$, b is the Burgers vector, $\overline{\rho}$ is the mean dislocation density, and μ is the shear modulus.

$$\mu = \mu_0\left(1 - 0.91 \times \frac{T - 300}{T_m}\right) \tag{3}$$

Here, μ_0 is the shear modulus corresponding to a temperature of 300 K, and T_m represents the melting point temperature. In the CA simulation $\overline{\rho}$ can be expressed as:

$$\overline{\rho} = \frac{1}{N_0}\sum_{i,j}^{i=A,j=B}\rho_{i,j} \tag{4}$$

where N_0 is the total number of cells in the CA model and $\rho_{i,j}$ is the dislocation density of the site (i,j).

During hot deformation, work hardening caused by deformation led to the proliferation of dislocation density, and softening caused by dynamic recovery and dynamic recrystallization resulted in the annihilation of dislocation density. The KM model[18] holds that dislocation density ρ and strain ε are related and this relationship is expressed as:

$$\frac{d\rho_{i,j}}{d\varepsilon} = k_1\sqrt{\rho_{i,j}} - k_2\rho_{i,j} \tag{5}$$

where k_1 is the effect of work hardening on dislocation density and k_2 is the effect of dynamic softening on dislocation density.

The critical dislocation density, $\rho_{cr,}$ can determine whether DRX nucleation occurs in CA simulations; ρ_{cr} can be calculated as:

$$\rho_{cr} = \left(\frac{20\gamma_i\dot{\varepsilon}}{3blM\tau^2}\right) \tag{6}$$

where γ_i is the large angle grain boundary energy, b is the Burgers vector, l is the mean free path of dislocation, τ is the energy of dislocation line per unit length, M is the grain boundary mobility.

2.3 Modeling of the grain growth

The grain boundary movement speed of the i^{th} recrystallized grain is expressed as follows[20]:

$$v_i = \lambda M f_i \tag{7}$$

where λ is the blocking migration parameter. 316LN steel is a single-phase steel, so λ is primarily related to the strain rate; f_i is the driving pressure acting on the

grain boundary, and M is the grain boundary mobility, which can be expressed as:

$$M = \frac{\delta D_{ob} b}{KT} \exp\left(-\frac{Q_b}{RT}\right) \tag{8}$$

where δ is the grain boundary thickness of the material, D_{ob} is the self-diffusion coefficient of the grain boundary at absolute zero, Q_b is the activation energy of grain boundary diffusion, and K is the Boltzmann constant.

Assuming that the new DRX grain is spherical, f_i can be expressed as:

$$f_i = \tau(\rho_m - \rho_i) - 2\frac{\gamma_i}{r_i} \tag{9}$$

where ρ_i and r_i are the dislocation density and radius of the ith recrystallized grain, respectively, ρ_m is the dislocation density of the matrix material, and γ_i is the interfacial energy, which is determined by the orientation difference between two adjacent grains.

$$\gamma_i = \begin{cases} \gamma_m & \theta_i \geq 15° \\ \gamma_m \frac{\theta_i}{\theta_m}\left(1 - \ln\frac{\theta_i}{\theta_m}\right) & \theta_i < 15° \end{cases}$$

Here, θ_i is the orientation difference between the recrystallized grains and the adjacent grains, θ_m and γ_m are the orientation difference and grain boundary energy of the large angle grain boundary, respectively. The value of γ_m can be calculated using the following equation:

$$\gamma_m = \frac{\mu b \theta_m}{4\pi(1-\nu)}$$

where ν is the Poisson's ratio.

2.4 Procedures of the simulation

The simulation in this study utilized the cellular automaton method, which involved discretizing a two-dimensional computational domain into square cells. The von Neumann neighbor type was utilized to simulate the equiaxed growth of recrystallized grains, focusing on the impact of the four closest neighboring cells on the central cell state. Each cell was assigned four state variables for calculation, including dislocation density, orientation, grain boundary, and recrystallization fraction, as well as three structural variables for statistical purposes, such as grain number, color and recrystallization time. The dislocation density variable represented the deformation storage energy of grains, while the grain boundary variable was used to record whether the cells were located at grain boundaries or within grains. In this simulation, the two layers of cells at the grain boundary were taken as grain boundaries, and the recrystallization fraction variable represented the proportion of recrystallization occurring in each cell. This can be calculated using the following equation:

$$f_i^t = \frac{\int_0^t v_i \, dt}{l_0} \tag{10}$$

where f_i^t is the recrystallization fraction of a cell (i, j) at time t, and l_0 is the unit length of a cell. In this simulation, l_0 = 2 μm. If a cell became a recrystallized nucleus, the recrystallization fraction variable of that cell was 1. Each dynamically recrystallized grain had a unique grain number which was used to calculate the recrystallized grain size.

In the CA simulation of DRX, several conditions had to be satisfied for the cell state change (DRX):

1) The driving force for the grain growth was greater than 0, or $f_i > 0$.
2) A cell was located at the grain boundary, and cells were present within its von Neumann neighborhood that had a greater recrystallization number than its own.
3) The recrystallization fraction variable of the cell was 1.
4) After satisfying the above three conditions, the cell could undergo recrystallization transition using the probability of $P = m/4$. Here, m was the number of cells with the same orientation as their neighbors. Constant 4 represents the number of cells in the von Neumann neighborhood.

A flowchart of the CA simulation of the DRX process can be seen in **Figure 1**. The material and process parameters required to simulate the DRX process were input first, and all cells were assigned the initial values. In our work, the judgment of $\varepsilon \geq \varepsilon_{total}$ depended on the total number of cycles. The total number of cycles was established based on material parameters and hot working parameters. The minimum time required to grow a cell was chosen as the time step, Δt, of the model, which is the ratio of the cell size l_0 to the maximum grain boundary movement rate[21].

$$\Delta t = \frac{l_0}{v_{max}} = \frac{k_2^2 l_0}{M\tau k_1^2} \tag{11}$$

With Equation (11), $\tau = \mu b^2/2$ and the strain increment $\Delta\varepsilon_{CA} = \dot{\varepsilon} \cdot \Delta t$ could be calculated. The total number of cycles was calculated based on the total strain ε_{total}:

$$n_{CA\_dynamic} = \frac{\varepsilon_{total}}{\Delta\varepsilon_{CA}} \tag{12}$$

The change in the dislocation density within each cell was calculated based on the strain increment. When the increase in the dislocation density reached the critical dislocation density for dynamic recrystallization, recrystallization nuclei formed at the grain boundaries. Cells that met the four conditions for the recrystallization state transition underwent a state transition, resulting in the growth of recrystallized grains. After the deformation was complete, the recrystallization percentage, original grain size, recrystallized grain size, and total average

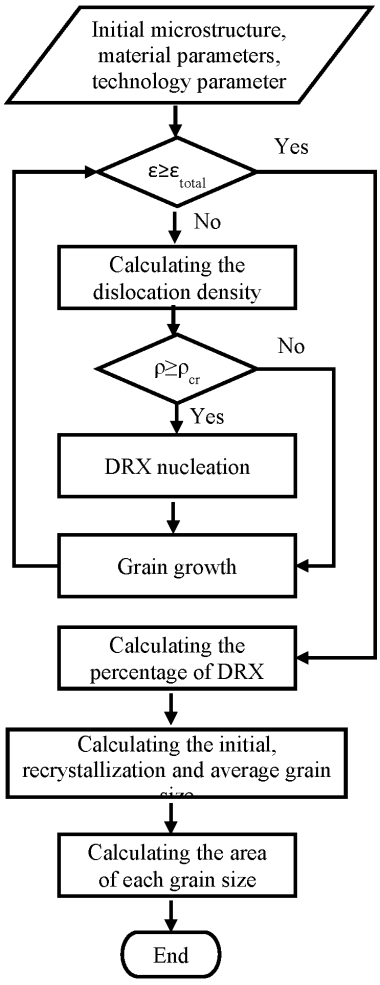

Figure 1: Flowchart of the CA model for the DRX process

grain size were calculated. The grain area for each degree of grain was counted to determine the grain size inhomogeneity coefficient. **Table 1** lists the key parameters used in this modeling.

Table 1: Key parameters used in the simulations

μ_0 (GPa)	v	Q_N (kJ mol^{-1})	D_{ob} (m^{2}s^{-1})	Q_b (kJ mol^{-1})	γ_m (J m^{-2})
77	0.28	467	5.6×10^{-10}	147	0.63

In this paper, CA simulations were used to study the grain distribution. If the research area is too small, it may not be representative of the actual grain distribution. In order to facilitate comparison with the later metallographic test data, an area of 2000 μm × 2000 μm was selected for the simulation. It was found through simulation experiments that excessively large cell sizes would reduce simulation accuracy and result in rough grain edges, which would not reflect the local characteristics of the material well. Conversely, using smaller cells would improve simulation accuracy, but increase the computing time and resources. To ensure accuracy and efficiency, the simulation area was divided into 1000 × 1000 cells, where each cell was equivalent to 2 μm × 2 μm. Simulations of the dynamic recrystallization process in metals were conducted using the MATLAB software. During the simulation process, custom MATLAB scripts were developed to define the simulation parameters and algorithms necessary for capturing the key aspects of dynamic recrystallization. On average, a single simulation took approximately 3 h. Throughout the simulations, the progress was monitored and relevant data were recorded for further analysis.

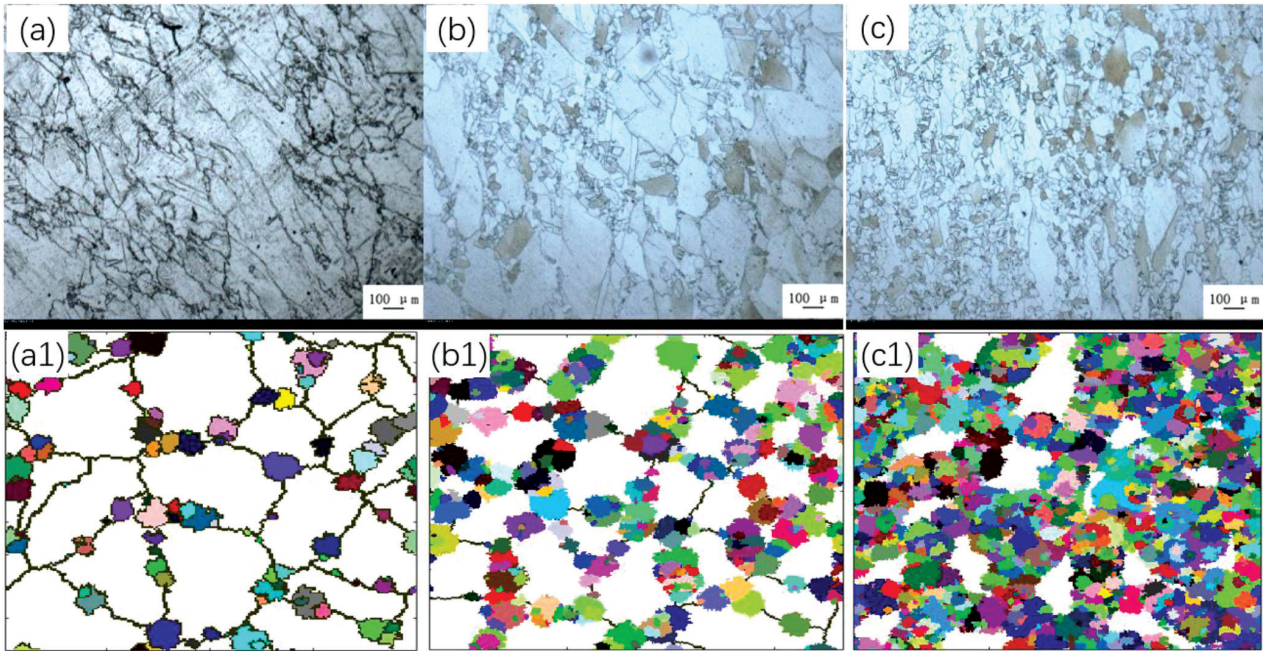

Figure 2: Experimental metallographic images and CA simulation results under different reduction rates (a forging temperature of 1200 °C; a deformation rate of 0.1s^{-1}), Metallography: a) 20 %, b) 30 %, c) 40 %, CA simulation: a1) 20 %, b1) 30 %, c1) 40 %

3 EXPERIMENTAL WORK

A thermal simulation test was conducted on 316LN austenitic stainless steel using a Gleeble-1500D simulation tester. The material was processed into standard samples with a size of $\varphi 8 \times 12$ mm prior to compression.[14] The experimental procedure involved heating a sample to 1250 °C at a rate of 10 °C/s, holding it for 3 min, cooling it to 1200 °C at 5 °C/s, and holding it for 60 s to eliminate any internal temperature gradient. Subsequently, hot compression was performed at a strain rate of 0.1 s^{-1}, with total compressive deformations of 20 %, 30 % and 40 %. After the completion of hot compression, the sample was immediately subjected to water cooling treatment.

Metallographic images and CA simulation results of the DRX process under the same process parameters are presented in **Figure 2**. It was observed that the CA simulation results were in good agreement with the experimental results, indicating the accuracy of the CA simulation. As the deformation increased, the recrystallization zones also increased. At a reduction rate of 20 %, few dynamically recrystallized nuclei were observed at the grain boundaries. When the reduction rate was increased to 30 %, the DRX zone expanded and the recrystallized

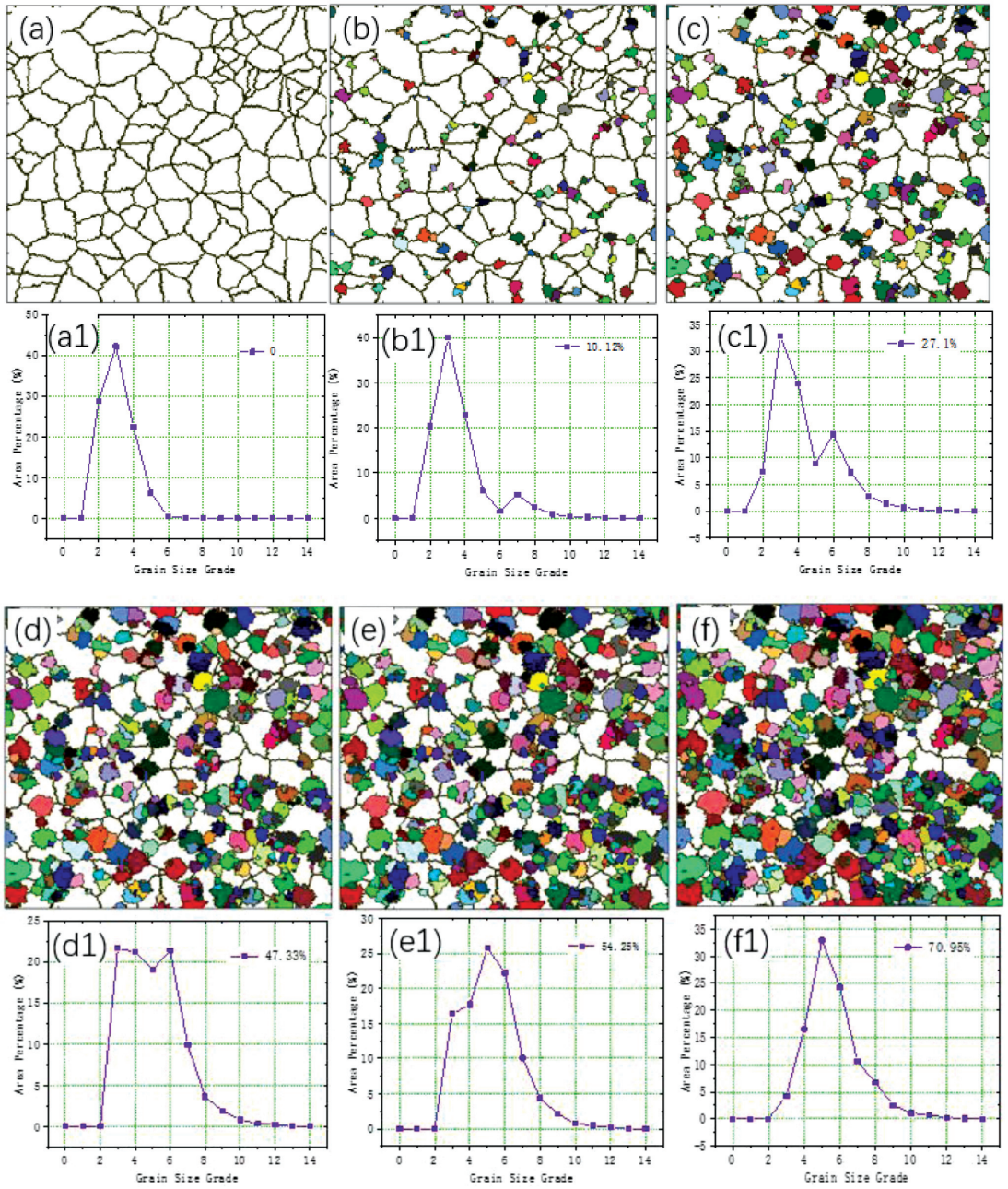

Figure 3: CA simulation results and grain distribution at different DRX percentages (a forging temperature of 1200 °C; a deformation rate of 0.1 s^{-1}): (a)(a1) 0 %; (b)(b1) 10.12 %; (c)(c1) 27.1 %; (d)(d1) 47.33 %; (e)(e1) 54.25 %; (f)(f1) 70.95 %

grains concentrated at the grain boundaries began to grow. At a reduction rate of 40 %, the DRX area increased to 70 %. Recrystallization occurred again in the recrystallization zone, resulting in continuous refinement of the grains and an increase in the average grain size.

The CA simulation results provided a clear and detailed visualization of the changes in the grain size at different stages of DRX. The simulation also enabled the calculation of important parameters such as the DRX area, recrystallization percentage and grain size distribution. Throughout the DRX process, the grain size distribution underwent several stages of inhomogeneity, including the ALA stage, wide differential stage, bimodal stage, cross-sectional stage and necklace stage.

The CA simulation results for the DRX of 316LN steel are shown in **Figure 3**, for a forging temperature of 1200 °C and a deformation rate of $0.1 s^{-1}$, along with the grain distribution at different DRX percentages. Without recrystallization, the initial grain size was concentrated in grade 2–5, and the area distribution showed a typical unimodal pattern. At 10.12 % DRX, dynamically recrystallized grains appeared, the grain size grade increased (the minimum was grade 12) and the area accounted for 6.67 %. The overall distribution of grain area had a bimodal pattern. The dominant grain size grade of big grains (the grains with the largest area) was 3, while the grade of small grains (dynamically recrystallized grains) was 7, yielding a grade difference of 4. At 27.1 % DRX, the dominant grade of big grains was still 3, but the area percentage decreased. The dominant grade of small grains was 6, and the occupied area increased. The distribution of grain area was bimodal. At 47.55 % DRX, the area of big grains continued to decrease and the area of small grains continued to increase. The area of grades 3–6 was almost the same, forming a wide differential pattern. At 54.25 % DRX, the initial grain area decreased and the total area of dynamically recrystallized grains increased alongside the progress of recrystallization. The distribution of grain area changed to a unimodal pattern. At 70.95 % DRX, the initial grain size decreased, the dynamically recrystallized grains continued to grow and the two grain sizes tended to be the same. At this point, the dominant grain size grade was 5, and the distribution of grain area showed the typical unimodal pattern. As DRX progressed, the initial grains continued to decrease, the grains recrystallized, the dominant grain size decreased and the average grain size decreased.

Figure 4 depicts the changes in the grain cross-sectional area and grain size grade in the CA simulation results for the DRX of 316LN steel. The trend of the change in the grain cross-sectional area was opposite to that of the grain size grade. As shown in **Figure 4b**, the average grain size grade of the original grains and the total average grain increased during the process of grain refinement. However, the average grain size grade of recrystallized grains decreased, reflecting the process of the nucleation and growth of dynamically recrystallized grains. In the early stages of DRX, the total average grain size grade was between the average grain size grade of the original grains and the average grain size grade of the recrystallized grains. Later in the process, the total average grain size grade was mainly determined by the average grain size grade of recrystallized grains. When the DRX percentage reached 70 %, the total average grain size grade was consistent with the average grain size grade of recrystallized grains.

4 NEW EVALUATION METHOD AND ITS APPLICATION

An evaluation method for the degree of grain size inhomogeneity using $\overline{D_{max}} / \overline{D_m}$ had been proposed previously where $\overline{D_{max}}$ represents the mean chord length of the largest grain and $\overline{D_m}$ represents the mean chord length of all the grains in a sample.[22] However, this method may

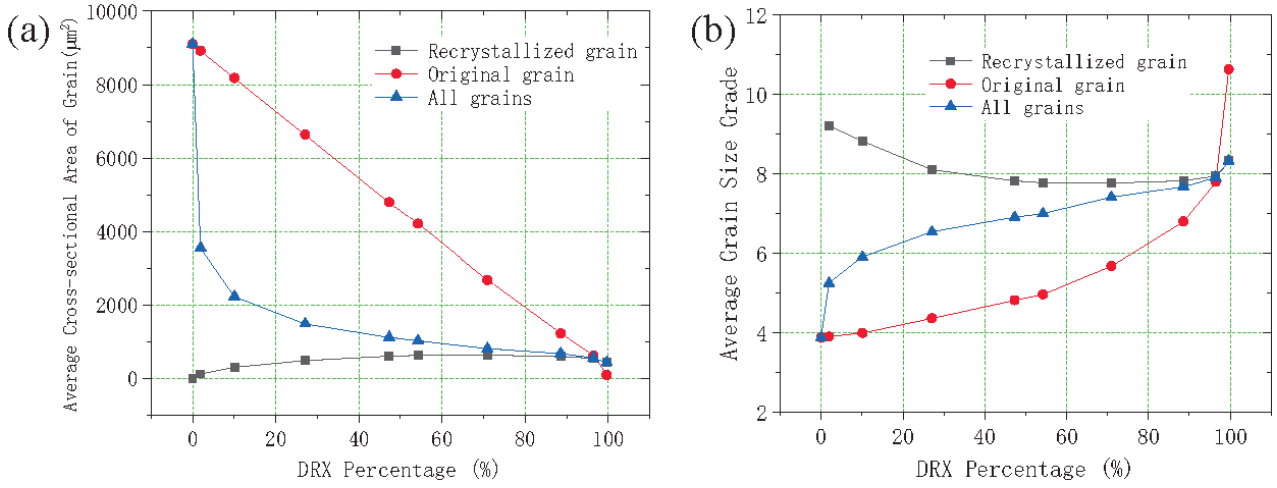

Figure **4:** Change in the grains during DRX throughout the CA simulation: a) changes in the average cross-sectional area of grains, b) changes in the average grain size grade

not accurately reflect the inhomogeneity as $\overline{D_m}$ contains $\overline{D_{max}}$, resulting in a higher proportion of the largest grain in the ratio. As a result, larger values of $\overline{D_{max}} / \overline{D_m}$ may lead to larger ratios and a more severe degree of inhomogeneity, which is not reasonable. An alternative method proposed by Chang et al. uses $\overline{D_{max}} / \overline{D_0}$ to evaluate the degree of grain size inhomogeneity where D_0 represents the average diameter of the grain grade with the highest frequency in the field of view.[23] However, this method intentionally ignores small-diameter grains and may not accurately reflect bimodal stages such as necklace stage, section stage and ALA stage.

In this paper, a new evaluation method of the grain size inhomogeneity was proposed. This method is suitable for unimodal and bimodal patterns, and can be described by the following equation:

$$G_u = G_m - (G_0 + A_0 / 2) \quad (8)$$

where G_u is the grain size inhomogeneity coefficient, G_m is the mean grain size grade, G_0 is the preponderant grain size grade, which is the largest area occupied by the grain size grade in the field of view, and A_0 is the area fraction of G_0.

G_u can simply and clearly allows an assessment of the grain size inhomogeneity in the field of view. The evaluation method is applicable to various states of the grain distribution. A higher G_u value indicates a greater degree of inhomogeneity, and this method is applicable to both unimodal and bimodal grain distributions. The average grain size can be easily obtained by calculating or measuring the preponderant grain size grate and its area fraction, while measurement errors have a minimal impact on the final result. Therefore, the G_u method is an accurate, easy-to-understand and practical way to evaluate the grain size inhomogeneity.

Different evaluation methods were used to evaluate the grain size inhomogeneity for different DRX percentages under the forging temperature of 1200 °C and deformation rate of 0.1 s^{-1}, as shown in **Figure 5**. Larger values obtained with these evaluation methods indicate a more severe inhomogeneity. **Figure 5a** shows that the G_u value increased rapidly when the DRX percentage was less than 47.3 %, which was consistent with the change in the grain distribution from unimodal to bimodal during DRX. When the DRX percentage was greater than 47.3 %, G_u increased and decreased repeatedly in a small range after a rapid decrease, reflecting the process of refining and homogenizing grains during DRX. As DRX is a dynamic process of continuous nucleation and growth, G_u increased and then decreased repeatedly. Overall, G_u increased and then decreased with the increase in the DRX percentage, and ultimately decreased, which aligns with the fact that DRX can refine and homogenize grains. Therefore, the G_u evaluation method accurately characterizes the state of the grain size inhomogeneity during DRX.

In **Figure 5b**, it can be observed that $\overline{D_{max}} / \overline{D_m}$ shows an increasing-decreasing trend with the increase in the DRX percentage. This method does not accurately reflect the effect of DRX on the grain refinement and homogenization. Similarly, **Figure 5c** shows that $\overline{D_{max}} / \overline{D_0}$ exhibits an overall increasing trend with the increase in the DRX percentage, which is contrary to observations. Therefore, these methods cannot accurately characterize the grain size inhomogeneity of the material. In contrast, the new method for evaluating inhomogeneity proposed in this paper, G_u, accurately characterizes the state of the inhomogeneity of materials.

A comparison between **Figure 3** and **Figure 5a** reveals that the G_u value of the initial grains was 0.67 before DRX commenced. As DRX progressed, new dynamically recrystallized grains were continuously generated, causing the mean grain size grade to rapidly increase. The grain size grade/area percentage curve exhibited a bimodal distribution (**Figure 3**) and G_u increased rapidly. When recrystallization reached 47.33 %, the grain size grade/area percentage curve exhibited a wide differential state, and G_u reached its maximum. At the 54.2 % recrystallization, DRX continued to nucleate, leading to grain refinement and an increase in the preponderant grain size grade, causing G_u to drop rapidly to 1.66. The grain size grade/area percentage curve returned to the unimodal state. As DRX progressed, the grains

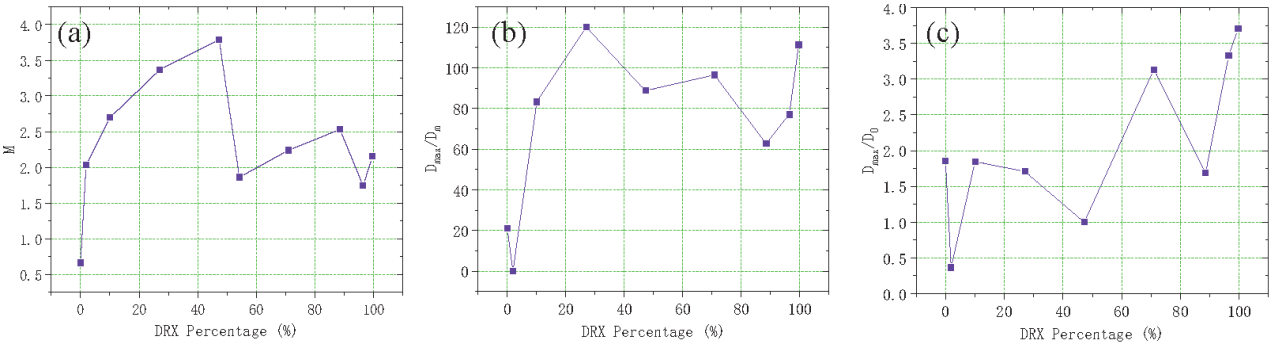

Figure 5: Different evaluation methods used to evaluate the grain size inhomogeneity during DRX: a) the new evaluation method, b) $\overline{D_{max}} / D_m$, c) $\overline{D_{max}} / D_0$

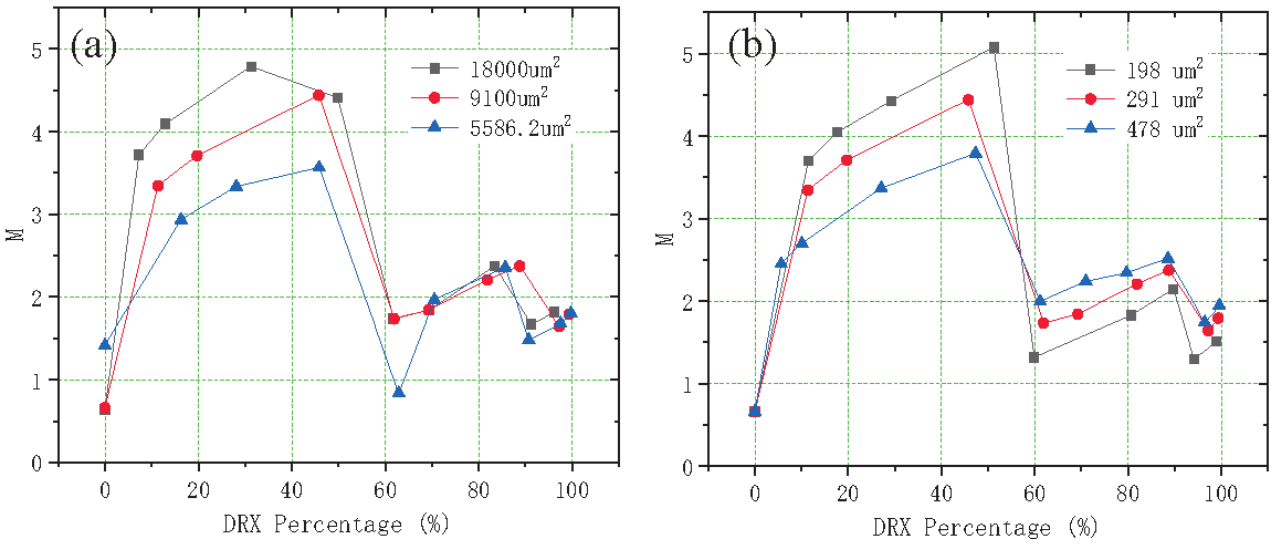

Figure 6: Changes in G_u during DRX with different initial grain sizes and recrystallization grain sizes: a) different initial grain sizes, b) different recrystallization grain sizes

continued to nucleate and grow, causing G_u to increase and decrease repeatedly within a small range until recrystallization was complete. Generally, the evolution of the grain size inhomogeneity during DRX can be divided into two stages. In the early stage of DRX, the grain size polarization is significant, and G_u shows an upward trend. The later stage of DRX is mainly the process of grain refinement, and G_u shows a downward trend. Since DRX involves repeated nucleation and growth when the degree of DRX is high, G_u becomes repetitive within a small range.

The new method for evaluating grain size inhomogeneity is useful for analyzing the evolution of grains during metal deformation and for studying the impact of different factors on inhomogeneity. **Figure 6a** displays the change in G_u during DRX with different initial grain sizes. The average cross-sectional areas of the initial grains were 18,000 μm², 9,100 μm² and 5,586.2 μm². The trend of G_u during recrystallization was the same for all the initial grain sizes, with an overall increase followed by a decrease, as seen in **Figure 6a**. When the DRX percentage was below 50 %, large initial grain sizes resulted in faster increases in G_u due to the greater size difference between the initial and recrystallized grains, and the more significant grain size inhomogeneity. However, when the percentage of DRX exceeded 50 %, the initial grains were fully refined, reducing the effect of the initial grain size on inhomogeneity. The values of G_u were similar and irregularities were present.

Figure 6b illustrates the changes in the coefficient G_u value during the DRX process with different recrystallized grain sizes. The average cross-sectional areas of the recrystallized grains were 198 μm², 291 μm² and 478 μm². When the DRX percentage was below 15 %, coefficient G_u increased rapidly. Since the recrystallized grains began to nucleate and did not grow in size, there was little difference in G_u even if there were different recrystallized grain sizes. When the DRX percentage was above 15 %, the recrystallized grains began to grow, and the growth rate of G_u slowed down. Coefficient G_u of the smaller recrystallized grains was larger. The main reasons for this were the facts that the size of the recrystallized grains was small, and the difference between the initial grain size and the recrystallized grain size was large, resulting in a larger G_u value. When the recrystallization percentage reached about 50 %, the initial grain area decreased, and the dominant grain grade increased as the recrystallized grains grew, leading to a sudden decrease in coefficient G_u. When the recrystallized area exceeded 50 %, coefficient G_u of the larger recrystallized grains was larger.

5 CONCLUSION

In this study, the cellular automation method was used to simulate the DRX of 316LN, and the resulting grain distribution was analyzed. A new method for evaluating the grain size inhomogeneity was proposed, introducing coefficient G_u to accurately and objectively measure the grain inhomogeneity.

Coefficient G_u was found to accurately reflect the changes in the grain size inhomogeneity during DRX. Regardless of the initial grain size, G_u showed an overall trend from an increase to a decrease during recrystallization. When the percentage of DRX exceeded 50 %, the effect of the initial grain size on inhomogeneity was reduced. Conversely, when the recrystallized area exceeded 50 %, the G_u coefficient of smaller recrystallized grains was smaller, indicating a more uniform grain distribution. In conclusion, the new evaluation method proposed in this study can accurately characterize the state of grain size inhomogeneity and is

applicable to various states of grain distribution. The G_u coefficient is easy to use and can be applied to analyze the grain evolution during a metal deformation and investigate the influence of different factors on inhomogeneity.

Future research will focus on applying the G_u coefficient to the simulation of large forgings. This will involve redeveloping the Deform software to include the G_u coefficient in the simulations, allowing for the prediction of grain non-uniformity during the formation of large forgings.

Acknowledgements

The work was financially sponsored by the National Natural Science Foundation of China (No. 51775361) and the Taiyuan University of Science and Technology Scientific Research Initial Funding (TYUST SRIF, No. 20212022).

6 REFERENCES

[1] Y. X. Jiao, J. S. Liu, X. W. Duan, et al., Prediction of critical forging penetration efficiency for 06Cr19Ni9NbN steel by dynamic recrystallization, Journal of Iron and Steel Research International, 24 (**2017**) 6, 83–87, doi:10.1016/S1006-706X(17)30097-3

[2] N. M. Ryabykin, Y. V. Protsiv, Grain Size Inhomogeneity in Ring Preforms Fabricated from High-Temperature Alloys, Metal Science & Heat Treatment, 43 (**2001**) 9–10, 351–355, doi:10.1023/A:1013636416379

[3] D. Feng, G. Wang, H. Chen, et al., Effect of grain size inhomogeneity of ingot on dynamic softening behavior and processing map of Al-8Zn-2Mg-2Cu alloy, Metals and Materials International, 24 (**2018**), 195–204, doi:10.1007/s12540-017-7324-2

[4] S. H. Sun, Y. Koizumi, S. Kurosu, et al., Phase and grain size inhomogeneity and their influences on creep behavior of Co–Cr–Mo alloy additive manufactured by electron beam melting, Acta Materialia, 86 (**2015**), 305–318, doi:10.1016/j.actamat.2014.11.012

[5] S. Y. Betsofen, A. L. Lapin, Inhomogeneity of Texture, Particle Precipitation and Grain Size under Recrystallization of Al-Mg, Al-Mg-Li and Al-Mg-Sc Alloys, Materials Science Forum, (2004), 363–368

[6] F. J. G. Landgraf, R. Takanohashi, et al., The origin of grain size inhomogeneity in semi-processed electrical steels, Journal of Magnetism and Magnetic Materials, 215 (**2000**), 92–93

[7] S. Nandi, B. K. Kar, P. P. Chaudhuri, Theory and Applications of Cellular Automata, IEEE Transactions on Computers, 43 (**1995**) 12, 1346–1357

[8] P. Alavi, S. Serajzadeh, Microstructural Changes during Static Recrystallization of Austenitic Stainless Steel 304L: Cellular Automata Simulation, Metallography Microstructure and Analysis, 9 (**2020**) 2, 223–238

[9] X. Z. Shi, S. W. Du, Static Recrystallization Mechanism of LZ50 Steel and Cellular Automata Simulation, 55 (**2019**) 14, 43–52, doi:10.3901/JME.2019.14.043

[10] F. Su, W. Liu, Z. Wen, Three-Dimensional Cellular Automata Simulation of the Austenitizing Process in GCr15 Bearing Steel, Materials, 12 (**2019**) 18, 3022, doi:10.3390/ma12183022

[11] T. Iwamoto, T. Sawa, S. Kubo, Constitutive Modeling of Single Crystal TRIP Steel Based on Transformation – Crystal Plasticity Theory and Computational Simulation of its Transformation and Deformation Behavior by Cellular Automata Approach, Journal of the Society of Materials Science Japan, 57 (**2008**) 3, 219–224, doi:10.2472/jsms.57.219

[12] M. Qian, Z. X. Guo, Cellular automata simulation of microstructural evolution during dynamic recrystallization of an HY-100 steel, Materials Science and Engineering A, 365 (**2004**) 1–2, 180–185

[13] P. Alavi, S. Serajzadeh, Simulation of recrystallization and martensite revision in 304L austenitic stainless steel after multi-pass rolling processes, Multiscale and Multidisciplinary Modeling, Experiments and Design, 3 (**2020**) 4, 227–244

[14] F. Chen, X. D. Zhao, J. Y. Ren, et al., Physically-Based Constitutive Modelling of As-Cast CL70 Steel for Hot Deformation, Metals and Materials International, 27 (**2021**), 1728–1738, doi:10.1007/s12540-019-00541-7

[15] F. Chen, K. Qi, Z. Cui, et al., Modeling the dynamic recrystallization in austenitic stainless steel using cellular automaton method, Computational Materials Science, 83 (**2014**), 331–340, doi:10.1016/j.commatsci.2013.11.029

[16] R. Ding, Z. X. Guo, Coupled quantitative simulation of microstructural evolution and plastic flow during dynamic recrystallization, Acta Materialia, 49 (**2001**), 3163–3175

[17] R. Ding, Z. X. Guo, Microstructural modelling of dynamic recrystallisation using an extended cellular automaton approach, Computational Materials Science, 23 (**2002**), 209–218

[18] H. Mecking, U. F. Kocks, Kinetics of flow and strain-hardening, Acta Metallurgica, 29 (**1981**), 1865–1875

[19] U. F. Kocks, H. Mecking, Physics and phenomenology of strain hardening: the FCC case, Progress in Materials Science, 48 (**2003**), 171–273

[20] C. Zhang, L. W. Zhang, The kinetics and cellular automaton modeling of dynamic recrystallization behavior of a medium carbon Cr-Ni-Mo alloyed steel in hot working process, Materials Science & Engineering, 678 (**2016**), 33–43

[21] G. Kugler, R. Turk, Modeling the dynamic recrystallization under multi-stage hot deformation, Acta Materialia, 52 (**2004**), 4659–4668

[22] M. Ma, T. Chang, Z. Gu, Discussion on Evaluation Method of Grain Size Inhomogeneity, Physics Examination and Testing, 1 (**1990**), 5–6

[23] T. Chang, M. Ma, Discussion on evaluation method of mixed crystal degree of steel, Physical Testing and Chemical Analysis, Part A: Physical Testing, 1 (**1989**), 40–41